Quantum beat spectroscopy in chemistry

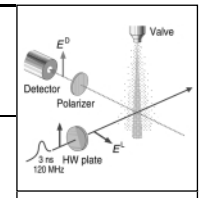

Robert T. Carter and J. Robert Huber

Physikalisch-Chemisches Institut der Universität Zürich, Winterthurerstr. 190, CH-8057 Zürich, Switzerland. Fax: +41-1-635-6838. E-mail: carter@pci.unizh.ch and jrhuber@pci.unizh.ch

Received 22nd March 2000
Published on the Web 10th August 2000

Quantum beat spectroscopy is a Doppler-free time domain method based on the creation of molecular coherences with a laser pulse and the measurement of their subsequent time evolution. Fourier transformation of the time evolution allows a spectrum in the frequency domain with lifetime-limited resolution to be recovered. This article gives an account of the technique applied in high resolution mode which allows the study of isolated molecules, radicals and complexes in extensive detail and with great accuracy.

1 Introduction

The structure and dynamics of molecular electronic states form a broad field of study with relevance to many areas of chemistry, such as the theory of molecular structure, dissociation, photodissociation, and reaction dynamics. The traditional tool of choice for study in this field has been high resolution spectroscopy, predominantly in the conventional frequency domain, where the absorption (or emission) is dispersed and recorded. With the development of the laser, high intensity, monochromatic and tunable light sources have become available, with bandwidths of < 1 MHz being routinely obtained from continuous-wave lasers. However, translating this bandwidth into spectral resolution is not trivial due to Doppler broadening caused by molecular motion and, for larger molecules, spectral congestion resulting from many quantum states being populated. A partial solution to these problems is to entrain the sample in a supersonic expansion of a buffer gas, allowing the molecule to be studied at very low temperatures. Typical rotational and vibrational temperatures are on the order of 5 and 50 K respectively, dramatically reducing spectral congestion. The translational temperature is even lower at ~ 1 K and results in pronounced narrower spectral lines. Reducing the linewidth to less than ~ 50 MHz at visible wavelengths is however still somewhat challenging. While this resolution may still be sufficient to learn a great deal about the structure of an electronic state, it may not be possible to discern small but important effects such as nuclear hyperfine splittings. Although techniques such as saturation spectroscopy and two photon methods are available to circumvent Doppler broadening, a simpler and more direct approach is possible, in which the time dependence of the system is observed following the coherent excitation (simultaneous excitation with a fixed phase relationship) of molecular states. This is quantum beat spectroscopy (QBS).

As its name implies, QBS is based on a quantum phenomenon: the preparation and subsequent time evolution of a coherent superposition of eigenstates. Quantum beat measurements are performed in a manner analogous to pulsed nuclear magnetic resonance (NMR) spectroscopy. In pulsed NMR, a short radio frequency pulse is used to excite nuclear spin states (resonances) and the time evolution of the excited spin states is recorded in the form of the free induction decay. A Fourier transformation is then performed, allowing the traditional frequency domain spectrum to be recovered from the time domain data. In QBS, energetically closely spaced levels are simultaneously excited with a short light pulse and the time evolution of the system is recorded, often as a fluorescence decay. The time evolution, which for fluorescence detection is an exponential decay, exhibits superimposed oscillations, the

Robert Carter was born near Manchester in 1968. After a childhood in the UK and Hong Kong, he studied chemistry at the University of Oxford, graduating in 1990. He subsequently stayed at Oxford to do research into the electronic spectroscopy of small radicals under the supervision of Professor John Brown and received his DPhil in 1993. He then joined Professor Huber's group in Zürich as a postdoc where he first encountered the quantum beat method. In 1997 he became an 'Oberassistent' and his present research interests include high resolution spectroscopy and molecular photodissociation.

Robert T. Carter

J. Robert Huber was born in Zürich, Switzerland. He studied chemistry at the Swiss Federal Institute of Technology (ETH) in Zürich and received his PhD from that institution in 1966. He was a postdoctoral fellow with the US Army Pioneering Research Laboratories in Natick, MA, and, afterwards, joined the faculty at Northeastern University in Boston. In 1973 he became Professor of Chemistry at the University of Konstanz, Germany, and in 1979 he assumed his current position as chaired Professor of Physical Chemistry at the University of Zürich. His research centers on molecular dynamics, laser spectroscopy and photochemistry.

J. Robert Huber

frequencies of which correspond to the energy splittings between the coherently excited levels. These are the quantum beats. Similar to pulsed NMR, the Fourier transform (FT) is taken to obtain the familiar frequency domain spectrum. As the frequencies of the quantum beats lie in the radio frequency range, the measurement is effectively Doppler-free.

The first quantum beats were independently observed by Aleksandrov,[1] and Dodd *et al.*[2] in 1964 in atoms using shuttered spectral lamps for excitation. In its first 15 years, QBS was almost exclusively applied to measurements in atoms in order to determine parameters such as g-factors and hyperfine structure. Reference 3 reviews these applications in more detail. Driven by the development of reliable tunable (dye) lasers and supersonic molecular beam methods, QBS was applied to the study of polyatomic molecules, in which quantum beats were first observed in 1979 by McDonald and coworkers.[4] The following years saw the application with nanosecond laser pulses to a number of molecular systems, reviews of which are available in the literature.[5,6] More recently, experimental developments have also allowed QBS to be applied to unstable polyatomic molecules and radicals, with the first work being published in 1996.[7,8] With the advent of pico- and then femtosecond lasers, ultrashort pulses have also been applied to QBS type measurements, particularly in work pioneered by Zewail and coworkers,[9] but with the exception of rotational coherence spectroscopy (RCS) the goal here has always been to achieve high temporal as opposed to spectral resolution. In other branches of the physical sciences, QBS has been used to study the physics of solid state samples,[10] and laser systems based on the quantum beat principle have been proposed.[11] It has also been applied to the investigation of the nature of molecular coherences themselves as well as their manipulation and response to fast perturbations,[12,13] motivated by the possible applications to selective chemistry and quantum computing.

The purpose of this review is to provide a general and up to date introduction to the application of QBS for high spectral resolution measurements. Older work, which has been discussed in other reviews,[5,6] will in general not be addressed here. The review is structured as follows: Sections 2 and 3 treat the theoretical background for QBS and the experimental setup required. The applications of QBS to the study of electronic excited states and vibrationally excited ground state levels are discussed in Section 4. As the coherence width of pico- or femtosecond laser pulses (5 GHz–10 THz) exceeds the typical Doppler width, in which case measurements can usually be made using conventional spectroscopic techniques, nanosecond laser pulses excitation is almost always used, an exception being the RCS technique discussed in Section 4.4. The applications are illustrated with a number of examples, mainly from our laboratory.

2 Theoretical aspects

In this section we provide a brief and simple account of the theory of QBS. For a more detailed treatment the reader is referred to previous reviews.[3,5,6] As an introductory remark, we note that an analogy may be drawn between quantum beats and the Young's double slits experiment, where the presence of two indistinguishable channels leads to interference effects. In the case of molecular systems monitored by fluorescence emission, insight into the time evolution of coherently excited states is provided by the four level system shown in Fig. 1. Initially the molecule occupies the state $|g\rangle$, while two closely spaced levels $|a\rangle$ and $|b\rangle$ are excited states energetically well separated from $|g\rangle$. The system is subjected to a light pulse resonant with the ground to excited state transition. If the coherence width of the light pulse, which is determined by the time–energy uncertainty $\Delta\nu \sim 1/(2\Delta t)$, exceeds the small energy difference between $|a\rangle$ and $|b\rangle$, $|E_a - E_b| = \hbar\omega_{ab}$, both transitions $|a\rangle \leftarrow |g\rangle$ and $|b\rangle \leftarrow |g\rangle$ are simultaneously excited, or more precisely coherently excited. For such a case of coherently excited levels $|a\rangle$ and $|b\rangle$, quantum mechanics tells us to write a superposition to describe the prepared state *i.e.*

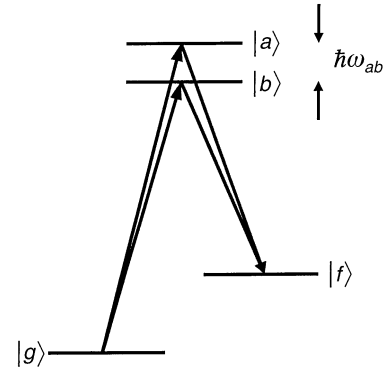

Fig. 1 Diagram of the four level system. A photon is absorbed by the ground state $|b\rangle$ and excites a superposition of states $|a\rangle$ and $|b\rangle$ whose energy separation is $\Delta E = \hbar\omega_{ab}$. Emission of a second photon leaves the system in the final state $|f\rangle$.

$$|\Psi(0)\rangle = c_a|a\rangle + c_b|b\rangle. \quad (1)$$

If the excitation intensity is constant over the range $\hbar\omega_{ab}$, then the coefficients c_a and c_b are proportional to the transition dipole matrix elements: $\mu_{ag} = \langle a|\boldsymbol{\mu}|g\rangle$ and $\mu_{bg} = \langle b|\boldsymbol{\mu}|g\rangle$, respectively. Having characterised the initial superposition state, we must now describe its time evolution. This is achieved with help of the time-dependent Schrödinger equation, the solution of which for the eigenstate $|a\rangle$ is for example $|a(t)\rangle = |a\rangle e^{-iE_a t/\hbar} = |a\rangle e^{-i\omega_a t}$. Applying this solution to the initial superposition state, we write its time evolution as

$$|\Psi(t)\rangle \propto \mu_{ag}|a\rangle e^{-(i\omega_a+\gamma_a/2)t} + \mu_{bg}|b\rangle e^{-(i\omega_b+\gamma_b/2)t}, \quad (2)$$

where the introduction of the phenomenological constants γ_a and γ_b accounts for the decay of states $|a\rangle$ and $|b\rangle$ respectively. It is now apparent that the system is described by two components oscillating at two distinct angular frequencies. We now assume that both levels $|a\rangle$ and $|b\rangle$ decay radiatively to the ground state level $|f\rangle$ so that the fluorescence intensity is given by the square of the transition dipole matrix element

$$I_{fl}(t) \propto |\langle f|\boldsymbol{\mu}|\Psi(t)\rangle|^2, \quad (3)$$

which after substitution of eqn. 2 can be evaluated as

$$I_{fl}(t) \propto |\mu_{ag}|^2|\mu_{fa}|^2 e^{-\gamma_a t} + |\mu_{bg}|^2|\mu_{fb}|^2 e^{-\gamma_b t} + |\mu_{ag}\mu_{bg}\mu_{fa}\mu_{fb}| e^{-(\gamma_a+\gamma_b)t/2} \cos(\omega_{ab}t + \theta). \quad (4)$$

Examination of this expression shows that it consists of two parts, one incoherent term (first two terms) describing the independent decays of the two states $|a\rangle$ and $|b\rangle$ and one coherent or cross term (last term) which decays at the average rate of the two states and, most importantly, is modulated at the angular frequency ω_{ab}. The modulation frequency is the difference of the two angular frequencies in eqn. (2), *i.e.* $\omega_{ab} = |\omega_a - \omega_b|$, and the coherent term in eqn. (4) is therefore termed the quantum beat. The angle θ is included in eqn. (4) to describe the phase of the quantum beat, which depends on a number of factors such as the excitation and detection polarisations and transitions. When the transition moments and decay rates are equal, as is often the case, a particularly simple expression is derived for the four level system. In this case eqn. (4) becomes

$$I_{fl}(t) \propto [1 + \cos(\omega_{ab}t + \theta)]e^{-\gamma t}, \quad (5)$$

clearly illustrating the contributions of the incoherent and coherent terms to the fluorescence decay. In this special case the quantum beat is 100% modulated. It is important to point out that the derivation above indicates that quantum beats are a

single particle phenomenon. As with the Young's slits experiment, averaged observation of a single atom or molecule would yield the same result as with an ensemble. This is an important difference to pulsed NMR where the relevant entity, the sample magnetisation, is an ensemble property.

Considering the Fourier transform of eqn. (4), we note that the product of two functions in the time domain yields the convolution of the two corresponding Fourier transforms in the frequency domain. As the Fourier transform of a simple exponential is a Lorentzian, the quantum beat will appear as a feature at frequency $\nu_{ab} = 2\pi\omega_{ab}$ with Lorentzian lineshape of full width half maximum (FWHM) $\nu_{\mathrm{FWHM}} = (\gamma_a + \gamma_b)/2$. This demonstrates that the resolution of QBS is limited only by the lifetime of the excited state levels and it is possible to increase the resolution even beyond this limit in favourable cases.[6] Fig. 2 illustrates the results with data obtained in our laboratory for Zeeman quantum beats in CS_2. As illustrated in the level diagram, the $M = \pm 1$ sublevels of a $J = 1$ rotational level in an electronic excited state were coherently excited (see Section 4.1). The fluorescence decay is clearly modulated at only one frequency, shown in the FT to lie at 1.05 MHz, corresponding to the energy splitting between the two M sublevels. Moreover the FWHM of the peak is 106 kHz, which corresponds to the excited state lifetime of 3.0 μs. The stronger feature at zero frequency is due to the unmodulated exponential terms in the fluorescence decay.

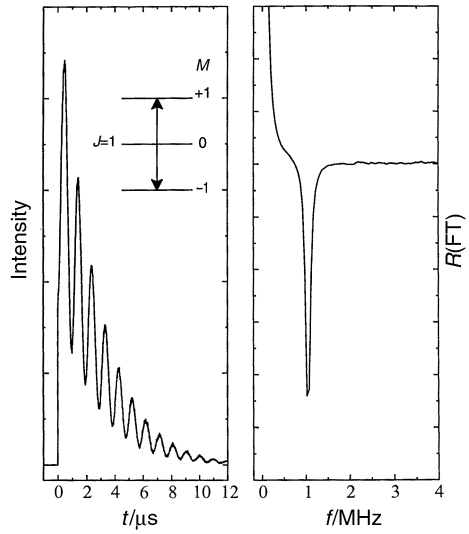

Fig. 2 Zeeman quantum beat recorded for the $R(0)$ line of the 17U transition in CS_2 in an external field of ~15 Gauss. The laser polarisation was perpendicular to the magnetic field direction and prepares a coherence between the $M = \pm 1$ sublevels as shown in the level diagram. This is manifested by a single quantum beat on the fluorescence decay; the real part of the Fourier transform is also shown. The less than 100% modulation, which is observed in virtually all quantum beat measurements in molecules, is due to incoherent emission from the excited states.

The treatment above considers a simple quantum beat system which is applicable to some atomic systems. For molecules, which have more degrees of freedom and thus a higher density of states, it is possible that a number of states may be coherently prepared, resulting in several quantum beats. If N levels are coherently excited, then $\frac{1}{2}N(N-1)$ quantum beats are possible (analogous to the number of handshakes among N people). Furthermore there may be more than one initial state and, particularly important for fluorescence detection, multiple detection channels to numerous final states. In order to adequately describe such systems, eqn. 4 must be adapted to include sums over the initial and final levels, and over the coherently excited states. A further complication is introduced by the possibility that the quantum beat phase θ varies over different detection channels. Hence in general, a density matrix formulation is used to model quantum beats in molecules. This has the advantage that it can also be applied to systems subjected to time-dependent perturbations. The reader is referred elsewhere for a description of these methods.[14] However, the bottom line is that providing a *pair* of states can be excited from a *common* ground state $|g\rangle$ and detection occurs to a *common* final state $|f\rangle$, a quantum beat is observed (*cf.* Fig. 1). If this is not entirely the case then incoherent emission accompanies the beat structure so that the latter is not 100% modulated. An instructive example is found in the fluorescence emission from the S_1 state of acetone. Incoherent excitation with no fixed phase relationship, which is usually applied, is followed by fluorescence decay with a 'boring' exponential form, however coherent excitation of many states yields the beautiful fluorescence decay and quantum beat spectrum shown in Fig. 3. In summary, QBS provides a simple and direct, Doppler-free method for measuring small energy differences between quantum states with lifetime-limited resolution.

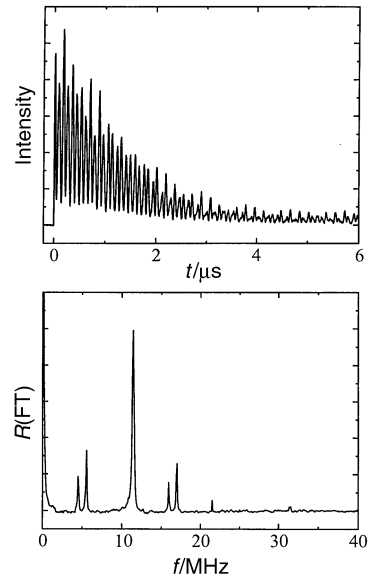

Fig. 3 Fluorescence decay and quantum beat spectrum recorded following coherent excitation of the $0_{00} - 1_{01}$ rotational line in the $23_0^{1+}I_{(0,0)}^{(3,0)}$ vibrational band of the $S_1 \leftarrow S_0$ transition in acetone. The quantum beats here are between eigenstates resulting from mixing between excited singlet and triplet state levels.

3 Experimental details

3.1 Basic requirements

The major obstacle to overcome in order to successfully record quantum beats is spectral congestion. Overlapped spectral features lead to a mixture of incoherently and coherently excited levels and hence a low modulation depth and many beat frequencies. For atoms and small diatomic molecules this is generally not a problem and quantum beat spectroscopy can be performed without special preparation, for example in the elemental vapour.[3] However in polyatomic molecules the room temperature spectra are too congested to allow individual transitions to be resolved and a cooled sample must be used. By using a supersonic expansion of a mixture of the sample seeded in a carrier gas, rotational temperatures of a few K may be achieved and simpler, well resolved spectra can be obtained. A pulsed jet is generally used to reduce sample consumption and demands on the vacuum pumps. A further advantage of a jet entrained sample is that collisions are minimised, reducing dephasing destruction of the molecular coherences.

In order to prepare coherences, the coherence width of the excitation light pulse must be of the order of the splittings to be

measured. For nanosecond lasers it is necessary to distinguish between the coherence width and spectral bandwidth. For example a standard commercial pulsed dye laser has a spectral bandwidth of 1–2 GHz but a pulse length of ~5 ns, corresponding to a coherence width of ~100 MHz. For dense spectra, spectral congestion problems may arise as the laser bandwidth is substantially larger than the coherence width. For the example above, two transitions separated by 400 MHz would not be resolved in the frequency domain. Recording the fluorescence decay of this single feature will yield the incoherent sum of two beat patterns, making analysis difficult. By applying Fourier transform limited pulses, this problem may be avoided (Section 3.2).

In detecting quantum beats, a technique is required which samples the time evolution of the excited coherences. Fortunately nature has provided such a mechanism in fluorescence decay. The simplest manner in which quantum beats can be detected is therefore to record fluorescence decay curves using a photomultiplier tube (PMT) and a transient digitizer or digital sampling oscilloscope. For molecules with a very low or zero fluorescence yield or for studies in the electronic ground state, a double resonance method is utilised, often in conjunction with the versatile resonance enhanced multiphoton ionisation (REMPI) technique. The REMPI method has the advantage of allowing convenient isotope specific detection when used with time-of-flight detection (see Section 4.5).

3.2 Experimental refinements

Fig. 4 shows a schematic of the experimental setup used in our group for the investigation of electronically excited states. The

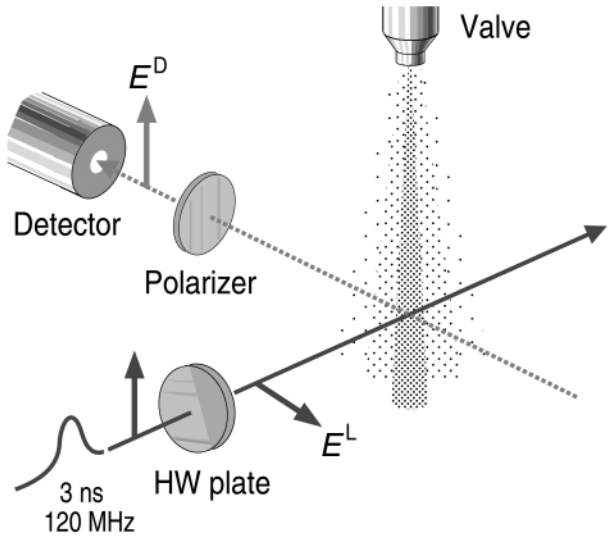

Fig. 4 A schematic of the apparatus used to take quantum beat measurements in electronically excited states. A molecular beam seeded with the sample is expanded into vacuum, where it crosses the excitation laser pulse and detection axis at right angles. The vacuum chamber is surrounded by three pairs of Helmholtz coils (not shown) to null the Earth's magnetic field. For measurements in which specific polarisations are required, a half wave (or quarter wave plate) and sheet polariser determine the excitation E^L and detection E^D polarisations, respectively.

sample is entrained in a pulsed supersonic molecular beam which is crossed at right angles by the excitation laser pulses. The fluorescence decay is detected in a direction mutually perpendicular to both sample and excitation beams. The most important refinement in our apparatus is the use of laser pulses with a Fourier transform limited bandwidth, *i.e.* having a spectral bandwidth equal to their coherence width, generated by an excimer pumped pulsed dye amplifier seeded by a ring dye laser. The pulses have a bandwidth of ~120 ± 15 MHz and a duration of 3.5 ± 0.5 ns following frequency doubling and allow the resolution problem discussed above to be overcome. With such excitation it is possible to move seamlessly from using the frequency domain to record spectral features split by more than 120 MHz to the time domain using QBS to record any splittings smaller than this value. This ability is particularly useful when studying larger molecules. Two other useful features can be seen in Fig. 4. A half wave or quarter wave retarder is available to generate specific linear or circular excitation polarisations for measurements where this is required. Similarly a sheet polariser allows the possibility of polarised detection. Our apparatus also incorporates three pairs of Helmholtz coils to null the Earth's magnetic field. For the generation of either static or switched magnetic or electric fields, Stark plates of Helmholtz coils can be built into the chamber.

Finally we note that many species of interest are unstable and require special experimental techniques to be produced in a supersonic jet. A number of possible methods have been suggested,[7,8] most of which involve the dissociation of a precursor at the start of the supersonic expansion. This yields the species of interest either directly or by reaction with another component of the gas mixture. The supersonic expansion stabilises and cools the molecule or radical so formed. Precursor dissociation is generally achieved either by laser photolysis, electrical discharge or pyrolysis. In our group we have used both the discharge and pyrolysis methods.

4 Application of QBS to chemistry

Before discussing the applications of QBS to molecules, it is useful to consider the possible origin of energy splittings which can be coherently excited by a nanosecond laser pulse, *i.e.* ~200 MHz or less and hence much smaller than rotational or vibrational structure. Two broad categories of phenomena are in general responsible. The first of these concerns the splitting of a single rovibronic level into subcomponents due to either effects internal to the molecule, such as nuclear hyperfine interaction or the application of external fields. Here QBS may be used to measure electric and magnetic dipoles, and nuclear hyperfine constants. These parameters yield information on the molecular and electronic structure of the molecule under study. Quantum beats in this category are characterised by their anisotropic nature, which is manifested by the dependence of their modulation and phase on the experimental geometry, *i.e.* the direction and polarisation of excitation and detection as illustrated in Fig. 5 for the case of Zeeman split hyperfine beats from $^{13}CS_2$. The anisotropic nature of these beats stems from angular momentum coupling considerations.[14] The second category deals with the coupling of a single rovibronic level in a 'bright' electronic state, to which transitions from the ground state carry oscillator strength, with rovibronic levels of 'dark' background states, to which transitions from the ground state carry no oscillator strength. These quantum beats are isotropic and have no dependence on the excitation and detection geometries. Their analysis yields information on the intramolecular dynamics mechanisms and the resultant energy flow. The discussion below starts with the applications of QBS in excited electronic states in Sections 4.1–4.3. Section 4.4 deals with picosecond excitation where the coherence width is ~10 GHz and hence allows coherent excitation of molecular rotational levels, while Section 4.5 treats the recent application of QBS to the electronic ground state.

4.1 Zeeman and Stark quantum beats

Applying an external magnetic or electric field lifts the degeneracy of the *M* sublevels *via* the Zeeman or Stark effects, which are dependent on the magnetic or electric dipole

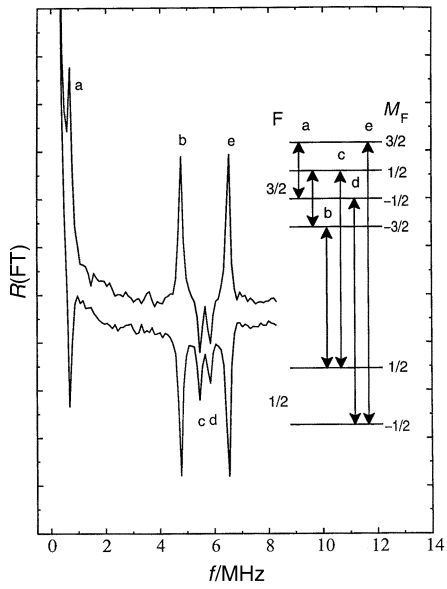

Fig. 5 Fourier transforms of fluorescence decays recorded for an $R(0)$ transition in the 10V system of $^{13}CS_2$ in the presence of an external field of ~6 Gauss directed along the laser propagation axis. The upper and lower traces were recorded with unpolarised detection but with laser polarisations parallel and perpendicular to the detection axis, respectively. The FTs show the anisotropic nature of Zeeman quantum beats (beat a) and Zeeman split hyperfine quantum beats (beats b–e), in that the beat phases depend on the experimental geometry.

moments, respectively. In general these splittings are small, and conventional spectroscopic techniques at optical frequencies require strong fields and large dipole moments to resolve the Zeeman and Stark components. The measurements may also be complicated by the presence of electric or magnetic dipoles in the upper and lower electronic states, which can make assignment difficult. In contrast QBS provides a method to directly measure the energy splittings between the M components in the excited state. This technique has the advantage that it is specific to the excited state and that much weaker fields may be used or, conversely, that smaller moments may be measured for a given field. Furthermore in the case of nonlinear interactions, as for the Stark effect, the beat frequencies are very sensitive to the rotational constants and provide a method to refine the values obtained from conventional spectroscopic methods and hence obtain a more accurate structure.[15] In order to prepare Zeeman or Stark coherences, states of different M must be coherently excited. Normally an experimental geometry is chosen in which the excitation (and detection) polarisation is perpendicular to the external field. In this case the selection rule for the M subcomponents is $M \pm 1 \leftarrow M$, preparing coherences with $\Delta M = 0, 2$. The $\Delta M = 0$ coherences normally have zero frequency while the $\Delta M = 2$ coherences yield the energy splittings between the M components.

One example of Zeeman quantum beats deals with the ultraviolet spectrum of CS_2.[16] The upper electronic state of the U system is the $\Sigma = 0$ component of a $^3A_2$ state and should therefore have no magnetic dipole moment, nevertheless rovibronic levels in this state are found to exhibit Zeeman splittings. At the fields used in the study (~1 mT ≡ 10 Gauss), the Zeeman effect is linear and the M sublevels experience a energy shift[5] of

$$E_Z = g_J \mu_B B M, \qquad (6)$$

where g_J is the Landé g-factor of the level in question, μ_B is the Bohr magneton and B is the magnetic field strength, respectively. Fig. 2 gives a level scheme for a rotational state with $J = 1$ and shows the single coherence excited *via* a R branch excitation step. For states of high J, a number of $\Delta M = 2$ coherences are excited, but due to the linear Zeeman effect the beat frequencies are identical. Fig. 2 shows the single beat frequency on the fluorescence decay and the corresponding FT. By measuring the dependence of the beat frequency on the field strength, the g-factor of the excited rovibronic level is obtained. Important to note is the very high resolution of the method: the beat frequency of only 1.05 MHz is very well resolved in the FT and g-factors as small as $g = 0.02$ can easily be measured with fields of only ~15 Gauss. In this study, analysis of the rotational state dependence of the g-factor on rotational quantum number J, revealed the origin of the excited state magnetic moment. This is the *spin uncoupling mechanism*, in which interaction between the rotational and electron spin angular momenta mix states with $\Delta\Sigma = 1$. Details of other recent work on Zeeman quantum beats may be found elsewhere.[17–19]

Stark quantum beats are measured in a similar manner, with an external electric field being applied instead of a magnetic field. However for an isolated state, the Stark shift is quadratic in field, in contrast to the linear low field Zeeman effect. For an singlet state rotational level, the Stark shift is given[5] by

$$E_s(J,M) = \sum_i (A_i(J) + B_i(J)M^2)\mu_i^2 E^2, \qquad (7)$$

where $A_i(J)$ and $B_i(J)$ are factors dependent on the molecular geometry, μ_i are the projections of the dipole moment on the principal axes, and E is the electric field strength. Equation (7) shows that levels with the same absolute M remain degenerate and as a consequence for a rotational level J, $J(J-1)$ equally spaced Stark beats will be observed. For molecules where the electric dipole moment lies on one of the principal axes (*e.g.* linear or C_{2v} molecules), the dipole moment can be determined from measurements on a single rovibronic level. This has been performed for a number of such species and we refer to the previous reviews for a list.[5,6] Another recent study may be found elsewhere.[20] However a more complete example is provided by propynal, a molecule with C_s symmetry where Stark quantum beats were used to measure the electric dipole moment *and its orientation* in the S_1, state.[21] This was achieved by taking measurements on a number (as a rule of thumb at least as many as the number of components to be determined) of rotational levels. Propynal provides another interesting application for Stark quantum beats, the measurement of asymmetry doublet splittings.[22] In a near symmetric top such as propynal, these can be very small (a few MHz) but cannot be measured by QBS as the rotational selection rules prevent their coherent excitation. The Stark effect mixes the M sublevels of the asymmetry doublets and quantum beats between these levels become allowed. The effect is quadratic at very low fields but quickly becomes linear, and by measuring the field dependence of the quantum beat frequencies, the zero field asymmetry splittings can be very accurately determined.

4.2 Hyperfine quantum beats

As with the Zeeman studies, the use of QBS to investigate nuclear hyperfine structure in molecules is also derived from studies in atoms. Nuclear hyperfine structure arises from coupling of nuclear spin angular momenta **I** to the rotational angular momentum **J**. The common coupling mechanisms are either magnetic (interaction of nuclear and electron spins) or electric (interaction of nuclear quadrupole and electronic field gradients) in nature. For a molecule with a single nuclear spin, the total angular momentum in the molecule is written as the vector sum $\mathbf{F} = \mathbf{J} + \mathbf{I}$. Quantum beats can be detected after coherent excitation of multiple hyperfine levels and thus provide a convenient manner for measuring these splittings, which normally have a magnitude of 100 MHz or less. Consideration of the general optical selection rule $F \pm 1, F \leftarrow F$ for the excitation and detection steps reveals that $\Delta F = 2, 1, 0$

hyperfine beats may be observed. As the hyperfine interaction takes place within the molecular frame the polarisation dependence of hyperfine quantum beats differs somewhat from that for Zeeman and Stark beats. Accordingly the modulation of hyperfine quantum beats is found to be proportional to the second Legendre polynomial of the cosine of the angle θ between the excitation and detection polarisations $P_2(\cos\theta) = \frac{1}{2}(3\cos^2\theta - 1)$. This function has value 1 at $\theta = 0$ and -0.5 at $\theta = 90°$ and is zero at the magic angle 54.7°. Nuclear hyperfine structure is a very sensitive and direct probe of electronic structure and we illustrate the data that may be obtained from nuclear hyperfine quantum beats with two examples.

The first of these is the U system in CS_2 discussed above for the Zeeman quantum beats where the nuclear hyperfine structure of the ^{13}C ($I = 1/2$) substituted isotopomer was also investigated.[16] In this molecule each rotational level with $J \geqslant 1$ is split into two hyperfine components with $F = J \pm \frac{1}{2}$. This is illustrated in the level diagram in Fig. 5 for a state with $J = 1$ with $F = 3/2$, 1/2 (the presence of an external magnetic field further splits the M sublevels in this case). The splitting between the hyperfine levels was measured by QBS and its rotational state dependence confirmed the presence of the spin uncoupling mechanism discussed above. The second example shows how a comparison of the hyperfine structure in the $A^2\Sigma^+$ state of the OD radical and its van der Waals complex Ar·OD recorded by QBS was used to elucidate the nature of the bonding in the $A^2\Sigma^+$ state of the Ar·OD complex.[23] This state is anomalously strongly bound (~ 1000 cm^{-1}) although the $X^2\Pi$ electronic ground state is 'normal' for a van der Waals complex. The reason for this had long been considered to be analogous to that for the exciplexes such as XeCl or ArF, which are bound in the excited state but not in the ground state (hence their efficiency as a laser medium). The deuteron has spin $I = 1$ and its hyperfine structure is an excellent probe of the bonding in the complex, the geometry of which is ArDO despite the name. OD and Ar·OD were produced for this study using an electric discharge nozzle. Fig. 6 shows an example of the data obtained.

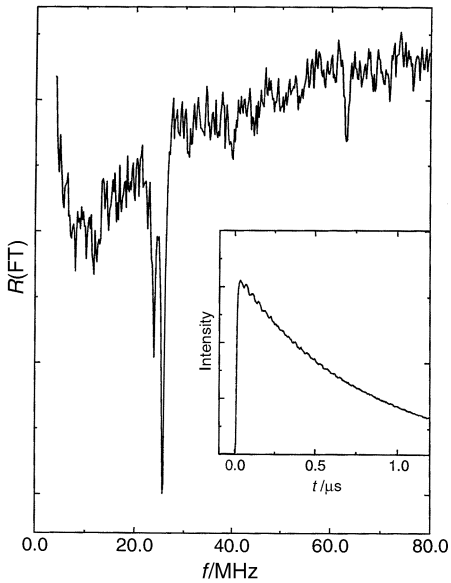

Fig. 6 Nuclear hyperfine quantum beats recorded for the $P_{21}/Q_1(3/2)$ line in a vibrational band of the $A^2\Sigma^+ - X^2\Pi$ transition in the Ar·OD van der Waals complex. The inset shows the fluorescence decay which exhibits weakly modulated quantum beats. Following Fourier transformation the beat frequencies between hyperfine levels in the $A^2\Sigma^+$ state are clearly visible.

Analysis of the hyperfine structure showed a number of coupling mechanisms to be active of which one is particularly simple to analyse. This is the Fermi contact term, a quantum phenomenon the strength of which is proportional to the unpaired electron spin density at the deuteron. The Fermi contact term was found to be 7% less in the complex than in free OD, indicating the donation of electron density from the Ar atom onto the OD moiety and confirming the chemical nature of the bonding in this electronic state of the Ar·OD complex.

Examples of other recent work on hyperfine quantum beats may be found elsewhere.[18,19,24,25] In addition, it is also possible to study the effect of external fields on nuclear hyperfine structure. The majority of studies have used external magnetic fields and an example recorded for the V system of $^{13}CS_2$ is shown in Fig. 5. Here the Zeeman split $F = 3/2$ and $F = 1/2$ hyperfine states for an excited state $J = 1$ level were coherently excited. The excitation/detection geometry was chosen so that $\Delta M_F = 0, 2$ coherences could be prepared. This allows Zeeman beats with $\Delta F = 0$, $\Delta M_F = 2$ (beat a), $\Delta F = 1$, $\Delta M_F = 0$ (beats c and d) and $\Delta F = 1$, $\Delta M_F = 2$ (beats b and e) to be observed as shown in the two FTs. The latter also illustrate the anisotropic nature of hyperfine beats in that they were recorded under identical conditions but with different excitation polarisations. In the case of more complicated hyperfine systems, the excitation/detection geometry is usually chosen so that only $\Delta M_F = 0$ beats are observed, splitting each zero field hyperfine beats into components of different M_F and allowing the g-factors of the excited states levels to be obtained. These are of interest as they yield further information on the nature of the structure of the excited electronic state, being sensitive to admixture of states of different multiplicity for example. Such measurements were performed in some detail for the OD/Ar·OD systems,[23] where they also allowed further refinement of the hyperfine parameters, as the Zeeman effect in this case becomes non-linear at very low fields.

4.3 Multilevel quantum beats

The examples above discussed the quantum beats obtained following excitation of components of a single rovibronic level. However another source of closely spaced levels is often active in polyatomic molecules: the coupling of levels in a bright electronic state with a manifold of dark background levels. Indeed it was for such cases that quantum beats were first detected in molecules.[4] The most studied examples consist of molecules with a singlet ground state, although multilevel beats have also been detected in radicals.[8] For a molecule with a closed shell ground state the origin of these beats is as follows. The first excited singlet state S_1 has a companion triplet state T_1 lying lower in energy. For polyatomic molecules, the vibrational state density increases exponentially with energy so that the triplet state vibrational levels form a dense manifold at the energy of the S_1 origin. The isolated bright singlet state levels can then couple with this triplet state manifold, *via* the spin–orbit interaction, to form an envelope of closely spaced eigenstates. Three cases have been identified depending on the density of the triplet state levels and coupling strength,[26] of which the intermediate case is particularly well suited to study with QBS. Typical triplet state densities here are tens to hundreds of vibrational levels per wavenumber. Analysis of these quantum beats, which differ from Zeeman, Stark or hyperfine beats in that they are isotropic, yields information on the density and identity of the coupled states and the strength and nature of the coupling mechanism. Our examples of multilevel quantum beats can be split into two categories.

In the first the excited eigenstates are not so congested and discreet quantum beats can be observed in the FT. Here counting the quantum beats created over a given coherence width provides a simple method for estimating the number of coupled states as the number of quantum beats n_{QB} is related to the number of eigenstates N by $n_{QB} = N(N-1)/2 \sim N^2/2$. Furthermore the fluorescence decay rate yields the average eigenstate lifetime. In the case of the S_1 state of propynal[27] the rotational state dependence of the number of coupled states and

eigenstate lifetime was investigated and the results for 3 excited rovibronic states are shown in Fig. 7. The observed linear

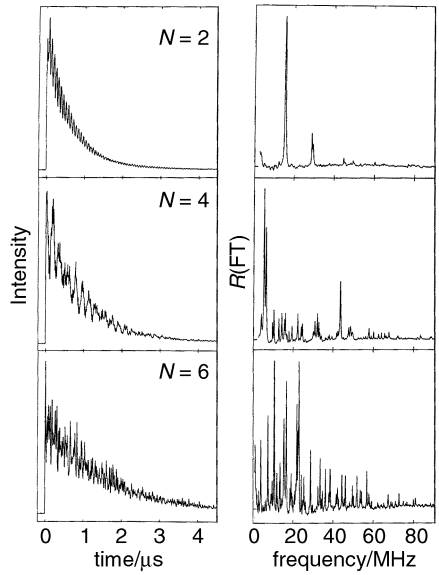

Fig. 7 Breakdown in the symmetry restrictions governing the coupling between a bright singlet state and dark triplet states in the $S_1 \leftarrow S_0$ electronic transition in propynal (HCCCHO). The three decays are from single rovibronic states with $J \equiv N = 2$, 4 and 6 which lie within an energy range of ~ 10 cm^{-1}. The corresponding FTs show a dramatic increase in the number of quantum beats (from 5 to 60) with rotational quantum number.

dependence of $n_{QB}^{1/2}$ with rotational quantum number $J \equiv N$ revealed a dramatic breakdown in the spin–orbit coupling symmetry restrictions due to mixing of states within the triplet manifold. The increase in triplet state admixture was also demonstrated by the observation of a correlated increase in the eigenstate lifetime with rotational quantum number. In another illustrative study, the dynamics of the S_1 state of acetaldehyde and its perdeuterated isotopomer were investigated.[28] For both species, quantum beat counting showed that the number of coupled states increased linearly with rotational quantum number J and the same behaviour was observed for the eigenstate lifetime data. A number of vibronic bands were investigated, right up to the dissociation barrier which is located on the T_1 potential energy surface. The work showed clearly that the T_1 manifold remains discreet up to the barrier and that the dynamics below this energy are governed by $S_1 \leftrightarrow S_0$ coupling. By following the eigenstate decay rates *versus* excess energy above the S_1 origin, the position of the dissociation barrier could be accurately located. These results are depicted in Fig. 8 and show a gradual increase in the decay rate with energy,

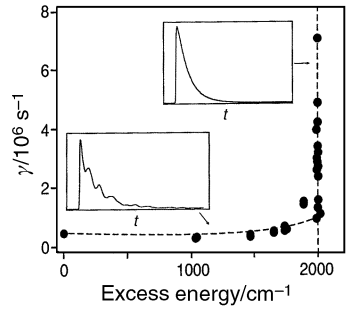

Fig. 8 The decay rates ($\gamma = 1/\tau$) of single rovibronic levels in the S_1 state of perdeuterated acetaldehyde (CD_3CDO) plotted against excess energy above the 0^0 level. A schematic of a typical delay at low excess energy, illustrating quantum beats due to mixing of singlet states with dark triplet states, is shown in the inset on the lower left. A barrier to dissociation lies on the triplet state surface at an excess energy of ~ 2000 cm^{-1}. Its presence is manifested by the rapid rise in decay rate; a schematic of a typical decay at this energy is shown in the inset at the top right.

terminated by a very rapid rise at the energy of the barrier itself. Above this energy the excited state dynamics are dominated by dissociation on the T_1 surface.

In the second category of multilevel quantum beats, the coupled states are so dense that discreet quantum beats can no longer be distinguished and the fluorescence decays take on a biexponential form (Fig. 9, bottom). This can be rationalised by

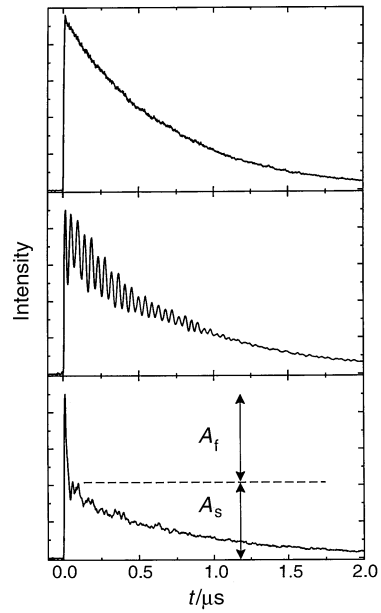

Fig. 9 Fluorescence decays recorded in the $6a_0^1 6b_0^2$ vibrational band of the $S_1 \leftarrow S_0$ transition in pyrimidine for different upper state rotational levels, from the left with $J = 0$, 2 and 5 respectively. Coupling of singlet and triplet levels results in eigenstates and the decays exhibit a transition in appearance from exponential (single eigenstate), through quantum beats (few eigenstates) to biexponential (many eigenstates). The arrows in the lower decay illustrate the concept of fast and slow components in a biexponential decay.

considering the time evolution of many multilevel quantum beats. Initially all beats are in phase and a large (coherent) signal is expected. However, the many beats of different frequencies rapidly begin to interfere destructively and the initial, coherent part of the signal falls off. Afterwards the form of the decay is determined by the (incoherent) emission of the individual eigenstates. Under these conditions, the form of the decay may be written as[29]

$$I(t) = A_f e^{-\gamma_f t} + A_s e^{-\gamma_s t}, \quad (8)$$

where the subscripts f and s represent the fast and slow decay components, respectively. As mentioned above γ_s is the average lifetime of the eigenstates, whereas γ_f is determined by the spectral width of the excited eigenstates. Furthermore the ratio of the two components A_f/A_s is proportional to the number of coupled eigenstates. An example where the analysis of biexponential decays provided detailed information on the intramolecular dynamics is for the S_1 state of pyrimidine,[30] results from which are displayed in Fig. 9. In this work the A_f/A_s ratio was found to increase linearly with J, showing the number of coupled states to increase with rotational excitation, paralleling the example above, also attributed to mixing within the triplet state manifolds. Analysis of the form of the fluorescence decays allowed the densities and lifetimes of the background triplet states to be estimated.

Thus careful analysis of multilevel quantum beats can yield useful information on the intramolecular dynamics and energy flow in molecular excited states. We note here that multilevel beats have been observed in a number of systems, recent examples include references 18, 19 and 31. Furthermore the effect of other factors on intramolecular dynamics such as internal rotation[32,33] has also been investigated.

4.4 Rotational coherence spectroscopy

We have stated that QBS is particularly useful when applied to the investigation of structures hidden within the Doppler linewidth and that it is more convenient to study features split by more than the Doppler width by conventional spectroscopic techniques. Since, however, rotational constants, which are fundamental parameters for molecular structure determination, scale inverse proportionally to the molecular size, it is clear that as the size of the molecule or molecular system to be investigated increases, a certain point is reached beyond which the rotational structure becomes so congested that it can no longer be resolved even in a cooled and skimmed molecular beam. Conventional methods utilise modeling of the rotational envelope to estimate the rotational constants of such systems, but a time domain method closely related to QBS using picosecond laser pulses could be a better choice. This is rotational coherence spectroscopy (RCS) developed by Felker and Zewail[34] on which we give a brief account below.

RCS is usually introduced with a semi-classical explanation based on the excitation of a transient alignment in the sample by a laser pulse, fast on the rotational timescale, and the observation of its subsequent recurrences due to the periodic nature of molecular rotation. However the theoretical treatment in Section 2 has prepared us to deal immediately with the quantum mechanics behind this phenomenon. The coherence width of a 50 ps laser pulse is 10 GHz and thus spans a substantial part of the rotational envelope in a large polyatomic molecule and hence excites many rotational transitions simultaneously. More specifically, the laser bandwidth is sufficiently broad to coherently excite multiple upper state rotational levels simultaneously from many ground state rotational levels. For the simplest case of a parallel polarised transition, the rotational selection rules are $J \pm 1$, $J \leftarrow J$ and $K \leftarrow K$ and for a given ground state level J, the following coherences between upper state rotational levels of the same K can be prepared: $(J-1) \leftrightarrow J$, $J \leftrightarrow (J+1)$ and $(J-1) \leftrightarrow (J+1)$. In the case of a prolate symmetric top, the angular frequencies of these coherences are $4\pi BJ$, $4\pi B(J+1)$ and $4\pi B(2J+1)$, respectively. Taking into account the multiple initial state levels, we see that many coherences are excited in the upper state, however their angular frequencies are all multiples of a single fundamental $\omega_0 = 4\pi B$. Time resolved detection of the system, which is most simply achieved using polarised fluorescence detection, will probe these coherences as rotational quantum beats. Extension of eqn. (4) shows that the fluorescence decay takes the form

$$I_{\mathrm{fl}} \propto \{A_0 + \sum_i [A_i \cos(n_i \omega_0 t + \theta)]\} \mathrm{e}^{-\gamma t}. \qquad (9)$$

Owing to the large number of rotational beats, the cosine terms above are generally out of phase and average to zero. However at times $t = 2m\pi/\omega_0$, where m is an integer, the term $\cos n_i\omega_0 t = 1$ for all i and hence a recurrence takes place as all rotational quantum beats regain the same phase. Similarly at times $t = (2m+1)\pi/\omega_0$ a partial recurrence takes place with some beats having positive and some negative phase. A more detailed treatment shows that these partial recurrences $t = (2m+1)\pi/\omega_0$ have opposite phases to the full recurrences at $t = 2m\pi/\omega_0$. The fluorescence decay therefore exhibits recurrences with alternating intensity and phase and a temporal spacing of $2\pi/\omega_0 = 1/2B$ between the full recurrences. Thus the rotational constant B can be obtained directly from the time resolved emission and the FT is not required for RCS. These recurrences are termed J-type and a simulation is given in Fig. 10. A pertinent example of this case is the stilbene molecule.[34]

If we now consider perpendicular polarised excitation and detection transitions, we see that the rotational selection rules $J \pm 1$, $J \leftarrow J$ and $K \pm 1 \leftarrow K$ allow the preparation of the coherences discussed above $\Delta J = 1, 2$; $\Delta K = 0$ as well as extra

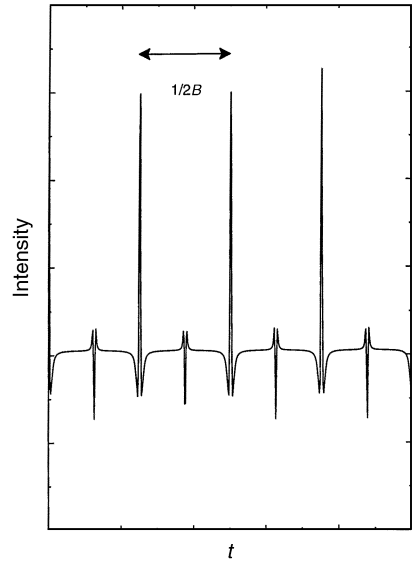

Fig. 10 A simulation of RCS measurements in a symmetric top showing J-type rotational recurrences. The sharp features arise from the presence of many simultaneously excited rotational quantum beats with frequencies which are a multiple of a single fundamental $\omega_0 = 4\pi B$. The spacing between the full recurrences is simply $1/2B$ (see text).

ones with $\Delta J = 0$; $\Delta K = 2$ and $\Delta J = 1, 2$; $\Delta K = 2$. The latter result in two new types of recurrence, K- and A-type, the spacings of which are given by $1/4(A - B)$ and $1/4A$ respectively. Thus if either K- or A-type recurrences can be observed in addition to J-type then both the rotational constants are obtained. For asymmetric tops the analysis of rotational coherences is somewhat more complicated. We refer the reader to reviews of the RCS method where detailed accounts of the analysis procedure can also be found and where structure determinations of small and large molecules, dimers and hydrogen bonded systems and clusters are presented.[34] It is worth noting that a number of detection techniques have been used for RCS in addition to fluorescence detection. These include pump–probe ionisation, in which one laser pulse pumps the state of interest and a subsequent second pulse probes it, and fluorescence depletion as well as time-resolved ionisation depletion methods. The latter two methods also have the advantage in allowing coherences in the ground state to be investigated.

4.5 Quantum beats in the electronic ground state

The examples above illustrate applications of QBS to the study of electronic excited states. However it is also most desirable to apply this method to the electronic ground state and in particular to vibrationally excited levels. The long lifetime of these states is attractive in that it results in excellent resolution in the FT. However a problem is posed here with the detection since IR emission is extremely weak and is difficult to record with sufficient temporal resolution. To overcome this problem we have applied the IR–UV double resonance method in the pump–probe mode. A home built IR optical parametric oscillator (OPO) is used to prepare coherences in a single rotational level of a selected molecular vibration. The time evolution of the coherences is then probed by scanning the delay of the UV probe pulse obtained from a dye laser and the signal is recorded after applying one of the following two modes. The first is excitation to an electronically excited level followed by fluorescence detection, while the second involves resonance enhanced multiphoton ionisation (REMPI) with detection of the ions so created. The sample in the double resonance work is also entrained in a supersonic expansion and a novel molecular beam/IR-pump beam geometry is employed. This allows the

time evolution to be measured over a long observation time (the vibrationally excited levels being very long lived) and dramatically increases the resolution in the quantum beat measurements. A more detailed description of the double resonance apparatus can be found elsewhere.[35] The data obtained using this technique is mainly of a spectroscopic nature as the examples below indicate, however it is clear that molecular dynamics can be explored as well. Examples in this context include the investigation of multilevel quantum beats in the electronic ground state arising from eigenstates formed by coupling discrete overtone levels with background levels which are of great interest to chemical dynamics but have yet to be detected.

In our first example, QBS in combination with an external electric field was used to measure the electric dipole moment in the $v_2 = 1$ state of propynal.[36] The recorded time evolution of the vibrationally excited state is shown in Fig. 11. The apparent

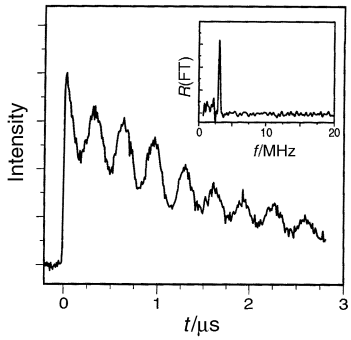

Fig. 11 Stark quantum beats recorded for the 2_{02} rotational level in the C–H stretch 2^1_0 vibrational band of the electronic ground state of propynal. The inset shows the FT. Studying the field dependence of the quantum beats for different rotational transitions, allows the magnitude *and* orientation of the molecular electric dipole moment in the $v_2 = 1$ level to be determined.

decay of the signal is due to movement of the sample and is a consequence of an older experimental geometry with collinear pump and probe beams. Inspection of Fig. 11 reveals a single deeply modulated quantum beat. The deeper modulation in the double resonance experiment is due to the use of single transition detection as opposed to the multiple detection channels in fluorescence detection. From analysis of the data, the magnitude and orientation of the electric dipole moment was obtained, allowing the dependence of the dipole moment on vibrational state to be assessed. The advantages of the QBS over conventional absorption in the ground state are similar to those mentioned for the electronically excited state (see above).

In the second example we examine the use of QBS for measuring hyperfine structure. Recent work in our group has demonstrated the use of the double resonance quantum beat method for measuring the nuclear quadrupole hyperfine splittings in vibrationally excited states of the diatomic HCl and the polyatomic molecule pyrimidine.[35] Fig. 12 shows the time evolution observed after coherently exciting the $v = 1$; $J = 1$ level of $H^{37}Cl$ as well as the corresponding Fourier transform. The time evolution demonstrates the deep modulation of the beats obtained by the double resonance method and clearly shows here the presence of two beat frequencies, which is confirmed in the FT. We note that the signal decreases much less than for the propynal results (Fig. 11) due to the novel molecular beam/pump beam geometry. The use of REMPI detection allowed results to be conveniently obtained for both $H^{35}Cl$ and $H^{37}Cl$ isotopomers and the quadrupole coupling constant eQq as well as the magnetic hyperfine parameter C_I(Cl) were determined with typical errors of 10–200 kHz. The pyrimidine system, results for which are also shown in Fig. 12, was studied using both LIF and REMPI detection. Owing to the lower beat frequencies in this case, the time evolution could be recorded over a substantially longer observation time than for the HCl measurements and consequently provided a superior resolution in the FT. Following analysis of the results, quadrupole coupling parameters with uncertainties between 10 and 20 kHz were obtained—an accuracy similar to that found in a microwave study. Furthermore this work showed that the time evolution of the IR excited levels can be recorded over a long observation window (at least over 60 μs), indicating that even a further improvement in the resolution is possible.

5 Conclusions

Quantum beat spectroscopy is a time domain method in which coherences are excited and their time evolutions are recorded. It

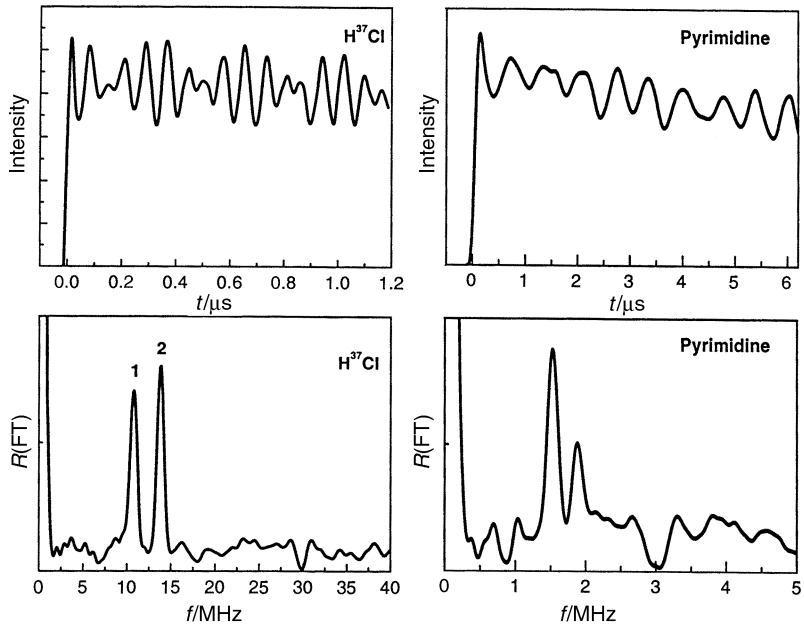

Fig. 12 Nuclear quadrupole hyperfine beats in the electronic ground states of HCl and pyrimidine. Upper panels: Time evolutions recorded for vibrationally excited levels of the S_0 states in $H^{37}Cl$ ($v = 1$; $J = 1$) and pyrimidine (C–H stretch $v_{13} = 1$; $J_{K_a,K_c} = 1_{10}$) using the pump–probe method with REMPI (left) and LIF (right) detection. Deeply modulated quantum beats are clearly visible. Lower panels: the real part of the FT of the time domain data.

is an essentially Doppler-free technique with a resolution limited only by the lifetime of the excited states, or more specifically the lifetime of the coherences. In this review we have discussed QBS in its high spectral resolution mode (< 100 kHz), where it is applied in conjunction with nanosecond laser pulses and is used to measure small splittings such as those between *M* sublevels whose degeneracy is lifted by the Zeeman or Stark effects, nuclear hyperfine levels arising from coupling of nuclear spin and molecular rotational angular momenta, and molecular eigenstates formed by coupling of a single bright level to a manifold of dark states. We have shown that QBS can be applied to both electronic excited states, usually in conjunction with fluorescence detection, and the electronic ground state using pump–probe double resonance method generally with REMPI detection. The analysis of quantum beat data, particularly when applied as a complementary method to conventional spectroscopic methods, allows extensive information to be obtained on a wide range of molecules, transient and radical species, and complexes. Examples include structural parameters such as magnetic and electric dipole moments, and magnetic and electric quadrupole hyperfine coupling constants, and quantities relevant to the study of intramolecular dynamics and energy flow such as state densities and coupling strengths. In considering future work, applications of QBS will include a broader investigation of radicals and transient species, energy flow in the electronic ground state particularly with respect to chemical dynamics and dissociation, and the application of QBS to novel systems such as molecular clusters and solid state samples.

In closing this review a few remarks on coherent excitation with ultrafast laser pulses, which may be regarded as the high temporal resolution mode of QBS, are appropriate. We have briefly discussed one aspect of this area in our account of RCS in Section 4.4 where picosecond laser pulses are used to coherently excite a manifold of rotational levels, the recurrences of which are used to extract structural parameters for systems ranging from molecules to clusters. More relevant to the broader chemical community is the use of femtosecond laser pulses, whose broad coherence width allows coherent excitation of molecular vibrational levels. This allows polyatomic molecules to be easily prepared in vibrational superposition states, which are often referred to as wavepackets, the time evolution of which can be followed by a second femtosecond pulse, using a pump–probe scheme. Such experiments allow bond fission and bond formation to be followed, opening the window for real-time observation of chemical dynamics. Indeed a pioneer of this work, Ahmed Zewail, received the 1999 Nobel prize for Chemistry in recognition of his seminal contribution to this exciting field.

6 Acknowledgements

The authors are indebted to past group members for their help in this work, in particular to Drs Herbert Bitto, Martin Dubs, Erwin Hack and Thomas Walther. Financial support of this work by the Schweizerischer Nationalfonds zur Förderung der wissenschaftlichen Forschung is gratefully acknowledged.

7 References

1 E. B. Aleksandrov, *Opt. Spectrosc. Engl. Transl.*, 1964, **17**, 522.
2 J. N. Dodd, R. D. Kaul and D. M. Warrington, *Proc. Phys. Soc.*, 1964, **84**, 176.
3 S. Haroche, in *High-Resolution Laser Spectroscopy*, ed. K. Shimoda, Springer, Berlin, 1976.
4 J. Chaiken, B. M. Gurnick and J. D. McDonald, *Chem. Phys. Lett.*, 1979, **61**, 195.
5 E. Hack and J. R. Huber, *Int. Rev. Phys. Chem.*, 1991, **10**, 287.
6 H. Bitto and J. R. Huber, in *Nonlinear Spectroscopy for Molecular Structure Determination*, ed. R. W. Field, E. Hirota, J. P. Maier and S. Tsuchiya, Blackwell Science, Oxford, 1998.
7 I. M. Povey, R. T. Carter, H. Bitto and J. R. Huber, *Chem. Phys. Lett.*, 1996, **248**, 470.
8 H. Kohguchi, Y. Ohshima and Y. Endo, *Chem. Phys. Lett.*, 1996, **254**, 397.
9 A. H. Zewail, in *Femtosecond Chemistry*, ed. J. Manz and L. Wöste, VCH, Weinheim, 1995.
10 H. Ohmura and A. Nakamura, *Phys. Rev. B: Condens. Matter*, 1999, **59**, 12216.
11 N. A. Ansari and M. S. Zubairy, *Phys. Rev. A: At., Mol., Opt. Phys.*, 1989, **40**, 5690.
12 H. Ring, R. T. Carter and J. R. Huber, *Eur. Phys. J. D*, 1998, **4**, 73.
13 H. Ring, R. T. Carter and J. R. Huber, *Eur. Phys. J. D*, 1999, **6**, 487.
14 K. Blum, *Density Matrix Theory and Applications*, Plenum Press, New York, 1981.
15 E. Hack, H. Bitto and J. R. Huber, *Z. Phys. D: At., Mol. Clusters*, 1991, **18**, 33.
16 D. T. Cramb, H. Bitto and J. R. Huber, *J. Chem. Phys.*, 1992, **96**, 8761.
17 P. Dupré, P. G. Green and R. W. Field, *Chem. Phys.*, 1995, **196**, 211.
18 N. Hemmi and T. A. Cool, *J. Chem. Phys.*, 1996, **105**, 7964.
19 D. A. Hostutler, T. C. Smith, H. Li and D. J. Clouthier, *J. Chem. Phys.*, 1999, **111**, 950.
20 N. Ohta and T. Tanaka, *J. Chem. Phys.*, 1993, **99**, 3312.
21 P. Schmidt, H. Bitto and J. R. Huber, *J. Chem. Phys.*, 1988, **88**, 696.
22 P. Schmidt, H. Bitto and J. R. Huber, *Z. Phys. D: At., Mol. Clusters*, 1987, **7**, 77.
23 R. T. Carter, I. M. Povey, H. Bitto and J. R. Huber, *J. Chem. Phys.*, 1996, **104**, 5365.
24 P. A. Hamilton, A. J. Phillips and R. Windsor, *Chem. Phys. Lett.*, 1997, **264**, 245.
25 H. Bitto, M. P. Docker, P. Schmidt and J. R. Huber, *J. Chem. Phys.*, 1990, **92**, 187.
26 M. Bixon and J. Jortner, *J. Chem. Phys.*, 1969, **50**, 3284.
27 H. Bitto, P. R. Willmott and J. R. Huber, *J. Chem. Phys.*, 1991, **95**, 4765.
28 T. Gejo, H. Bitto and J. R. Huber, *Chem. Phys. Lett.*, 1996, **261**, 443.
29 F. Lahmani, A. Tramer and C. Tric, *J. Chem. Phys.*, 1974, **60**, 4431.
30 R. T. Carter, H. Bitto and J. R. Huber, *J. Chem. Phys.*, 1995, **102**, 5890.
31 A. H. Zewail, *Ber. Bunsen-Ges. Phys. Chem.*, 1985, **89**, 264.
32 H. Bitto, *Chem. Phys.*, 1994, **186**, 105.
33 H. Bitto and S. Gfeller, *Chem. Phys. Lett.*, 1997, **265**, 600.
34 P. M. Felker and A. H. Zewail, in *Femtosecond Chemistry*, ed. J. Manz and L. Wöste, VCH, Weinheim, 1995.
35 H. Lammer, R. T. Carter and J. R. Huber, *Eur. Phys. J. D*, 2000, **8**, 385.
36 Th. Walther, H. Bitto and J. R. Huber, *Chem. Phys. Lett.*, 1993, **209**, 455.